Optik 124 (2013) 4353–4358

Contents lists available at ScienceDirect

Optik

journal homepage: www.elsevier.de/ijleo

Review on diode-pumped alkali vapor laser

F. Gao[a,b,*], F. Chen[a], J.J. Xie[a], D.J. Li[a], L.M. Zhang[a], G.L. Yang[a], J. Guo[a], L.H. Guo[a]

[a] State Key Laboratory of Laser Interaction with Matter, Changchun Institute of Optics, Fine Mechanics and Physics, Chinese Academy of Sciences, Changchun 130033, China
[b] Graduate School of the Chinese Academy of Sciences, Beijing 100039, China

ARTICLE INFO

Article history:
Received 15 August 2012
Accepted 6 January 2013

PACS:
42.55.Lt
42.55.Xi
42.60.By

Keywords:
Gas laser
Diode-pumped laser
Alkali vapor

ABSTRACT

Diode-pumped alkali vapor lasers (DPAL) are attracted much attention during recent years for its numerous potential applications. Development of DPAL is reviewed in this paper. The key techniques of DPAL are summarized and analyzed in detail, including the interactions between buffer gas and alkali vapor, pumping structure and power scaling magnification. Novel techniques used in DPAL are discussed, such as hydrocarbon-free DPAL and unstable cavity with transverse pumping. Blue-violet lasers by frequency doubling of DPAL are also introduced specifically. In addition, potential applications and the prospects of DPAL are concluded briefly.

1. Introduction

Efficient operation of a high-power laser with good beam quality is investigated for several decades for its wide applications in industry, medicine, military and sciences. Diode-pumped solid-state laser (DPSSL) [1–5] and chemical gas laser [6–9] are classical laser sources and they have been developed quickly. But plentiful hazardous gases used in chemical gas laser will limit its applications and remarkable thermal effect in DPSSL will restrict the improvement of its output power and beam quality. In recent years, diode-pumped alkali vapor laser (DPAL) has been paid much attention for its merits in high efficiency, high power, and good beam quality [10–24]. For example, the quantum efficiency and the stimulated emission cross-section are as high as $\eta_Q = 98.1\%$ and $\sigma_s = 5.4 \times 10^{-13}\ \mathrm{cm}^2$, respectively, by using 795 nm laser diode (LD) as pumping source of 780 nm Rb laser. And the refractive-index variation of He–Rb mixture gas under high operating temperature is only $dn/dT = 2.3 \times 10^{-10}/^\circ\mathrm{C}$. In addition, thermal management of DPAL is much better than DPSSL for the gaseous gain medium can be flowed. Therefore, output power of DPAL can be scaled up by increasing its oscillating volume and pumping power, and simultaneously the beam quality can be kept at high level. All these features indicate that DPAL can be a promising alternative of high power laser system.

At the beginning of the laser era, alkali vapor as laser gain medium had been investigated [25–27]. In the last two decades of last century, the amplified spontaneous emission (ASE) in alkali atoms was studied [28–31]. After entering the 21st century, DPAL has been developed rapidly with the development of high-power LD. The concept of DPAL [10] is firstly introduced by Krupke in 2001. Subsequently, Krupke's group demonstrated the first Rb laser [11] operating at 795 nm by using a Ti:sapphire laser as surrogate pumping source in 2003. After then, Rb laser pumped by LD arrays, in fact the first DPAL, was realized in 2005 [12]. Meanwhile, DPAL using Cs or K vapor as gain medium are also realized successively [13–16]. For the moment, the highest output power of reported DPAL was 145 W for continuous wave and 207 W for peak power at 14% duty factor [17], and the highest slope-efficiency was 81.7% [18].

In this paper, the development of DPAL is reviewed and the key techniques are summarized and analyzed in detail, including the interactions between buffer gas and alkali vapor, pumping structure and power scaling magnification. Novel techniques used in DPAL are discussed, such as hydrocarbon-free DPAL and unstable cavity with transverse pumping structure. Blue-violet laser by frequency doubling of DPAL is also introduced specifically. Additionally, potential applications and the prospects of DPAL are concluded briefly.

2. Key techniques of DPAL

Alkali vapor laser is a three-level laser system which is composed of the ground level $^2S_{1/2}$, the first excited level $^2P_{1/2}$ and the

* Corresponding author at: State Key Laboratory of Laser Interaction with Matter, Changchun Institute of Optics, Fine Mechanics and Physics, Chinese Academy of Sciences, Changchun 130033, China.
E-mail address: gaofei0104@163.com (F. Gao).

0030-4026/$ – see front matter © 2013 Elsevier GmbH. All rights reserved.
http://dx.doi.org/10.1016/j.ijleo.2013.01.061

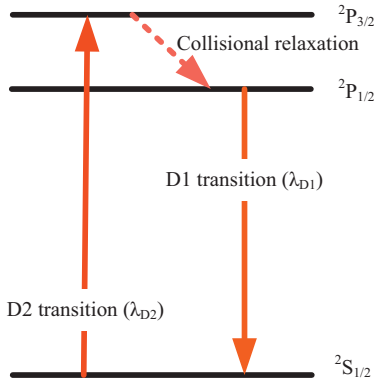

Fig. 1. Energy level diagram of the alkali vapor laser.

second excited level $^2P_{3/2}$, as shown in Fig. 1. The first and second excited levels are fine-structure levels split up by a relatively small energy due to spin–orbit interaction. The two resonance transitions $^2P_{1/2} \rightarrow {}^2S_{1/2}$ and $^2S_{1/2} \rightarrow {}^2P_{3/2}$ are called D1 transition and D2 transition corresponding to the lasing transition and pumping transition, respectively. As listed in Table 1, the quantum efficiencies of alkali vapor lasers are very high for the energy defects between D1 and D2 transition are quite small. It is indicated that the energy transfer from pumping source to alkali vapor laser is effective and less waste heat is generated in the gain medium. Therefore, the alkali atoms have the potential of efficient laser operation.

2.1. Interactions between buffer gas and alkali vapor

Buffer gas is used to improve the performances of alkali vapor laser, such as broadening the absorption line-width homogenously and fastening the fine-structure mixing rate and so on. Although buffer gas has important impacts on DPAL, but it is observed that chemical contaminations appear on the gain cell windows as DPAL is operating constantly at high temperature. To avoid the contaminations and ensure the operating stability, novel type named hydrocarbon-free DPAL has been developed recently.

2.1.1. Line-width broadening of D2 transition

Without buffer gas, the spectral character of D2 transition is determined essentially by Doppler-broadening with a Gaussian line-shape. The line-width is given by

$$\Delta\nu_D = 7.16 \times 10^{-7} \left(\frac{c}{\lambda_{D2}}\right) \left(\frac{T}{M}\right)^{1/2} \quad (1)$$

Here T is the operating temperature in Kelvin; M is the atomic mass of alkali atom. The Doppler line-widths of D2 transitions for K, Rb and Cs atom are listed in Table 2.

Compared with the typical spectral width of commercial diode-laser, the Doppler line-width is quite narrow and the Doppler broadening D2 transition is inhomogeneous. In order to absorb the pumping power of LD efficiently, the D2 transition must be broadened sufficiently. It can be realized by adding a partial pressure of buffer gas like helium. Collisions of the alkali atoms with the buffer gas atoms will broaden and reshape the D2 transition. When the buffer gas collision is in domination, the spectrum of D2 transition becomes Lorentzian line-shape, and the transition is broadened homogeneously.

The Lorentzian line-width of D2 transition with the buffer gas of He is given by

$$\Delta\nu_L = \gamma_T n_{He} \quad (2)$$

Here γ_T is the alkali-He collisional broadening coefficient, its value is measured by experiments; n_{He} is He number density in unit of amg (1 amg = $2.69 \times 10^{19}/\text{cm}^3$). The measured values of γ_T [19] are listed in Table 3.

To obtain a certain value of $\Delta\nu_L$, the pressure of He injected into the gain cell is calculated by

$$P_{He} = P_0 n_{He} \left(\frac{T}{T_0}\right) \quad (3)$$

Here T_0 = 273.15 K, P_0 = 1 atm, and T is the temperature of gas mixture corresponding to its partial pressure. For the typical collisional line-width value of 12 GHz [16,23,32,33], the pressure of He is listed in Table 3.

Additionally, the D1 transition is also broadened homogeneously with He, which means that the laser transition is induced without spatial hole burning.

2.1.2. Fast mixing of fine-structure energy levels

During the lasing process of DPAL, the alkali atoms are cycling the photons from LD through pumping transition $^2S_{1/2} \rightarrow {}^2P_{3/2}$, fine-structure mixing $^2P_{3/2} \leftrightarrow {}^2P_{1/2}$ and lasing transition $^2P_{1/2} \rightarrow {}^2S_{1/2}$. In some theoretical models on DPAL [34,35], the mixing rate between fine-structure levels $^2P_{3/2}$ and $^2P_{1/2}$ is supposed to be infinite, and the DPAL is operating as a quasi-two level system in this assumption. But in fact, the fine-structure mixing is the slowest step in the cycle, and will limit the cycling rate. Thus, population excited to the level $^2P_{3/2}$ must be relaxed to the upper laser level $^2P_{1/2}$ at a fast rate once the pumping energy is efficiently absorbed.

The fine-structure mixing rate can be varied by adding another molecule gas like ethane, namely the spin-mixing gas. In this approach, the fine-structure mixing rate due to the inelastic collisions between alkali atoms and ethane molecules is given by [36]

$$\gamma_{^2P_{3/2} \rightarrow {}^2P_{3/2}} = n_{C_2H_6} \sigma_{^2P_{3/2} \rightarrow {}^2P_{3/2}} v_r \quad (4)$$

Here $n_{C_2H_6}$ is the number density of ethane in the gain cell; $\sigma_{^2P_{3/2} \rightarrow {}^2P_{3/2}}$ is the cross-section of alkali atoms for ethane; v_r is the relative thermal average velocity between alkali atoms and ethane molecules, which is given by

$$v_r = \left[3k_B T \left(\frac{1}{m_{alkali}} + \frac{1}{m_{C_2H_6}}\right)\right]^{1/2} \quad (5)$$

Table 1
Atomic parameters of alkali vapor laser.

Alkali atom	λ_{D2} (nm)	λ_{D1} (nm)	Energy gap ($^2P_{3/2} \rightarrow {}^2P_{1/2}$) ($\text{cm}^{-1}$)	Quantum efficiency
K	766.70	770.11	57.7	99.5%
Rb	780.25	794.98	237.9	98.1%
Cs	852.35	894.95	554.1	95.2%

Table 2
Doppler line-widths of D2 transitions for K, Rb and Cs at 373 K.

Alkali atom	Atomic mass	$\Delta\nu_D$ (GHz)
K	40	0.852
Rb	85	0.569
Cs	133	0.419

Table 3
Measured values of γ_T and P_{He} for different alkali atoms at 373 K.

Alkali atom	γ_T (GHz amg^{-1})	$\Delta\nu_L$ (GHz)	P_{He} (atm)
K	26.7	12	0.614
Rb	18.6	12	0.881
Cs	21.7	12	0.755

Table 4
Development of hydrocarbon-free DPAL.

Researcher, year, institute	Alkali	P_{He} (atm)	P_{out}	η (%)	T (°C)
S.S.Q. Wu, 2008, LLNL [32]	Rb	2.7	130 mW	7	145
J. Zweiback, 2009, GAAS [23]	K	2	9 mJ	57	197
J. Zweiback, 2010, GAAS [33]	Rb	2.8	28 W	2	139
J. Zweiback, 2011, GAAS [38]	K	3	32 mJ	53	205

Table 5
Development of transverse pumping alkali vapor laser.

Research, Year, Institute	Alkali	P_{out}	η (%)
B.V. Zhdanov, 2008, USAFA [22]	Cs	28 W	15
B.V. Zhdanov, 2009, USAFA [15]	Cs	49 W	49
J. Zweiback, 2011, GAAS [38]	Rb	40 mJ	75
	K	32 mJ	53

Here k_B is the Boltzmann constant; m_{alkali} and $m_{C_2H_6}$ is the mass of alkali atom and ethane molecule, respectively.

2.1.3. Hydrocarbon-free DPAL

With the buffer gas of ethane, enough inversion population of alkali laser can be obtained. However, chemical reaction between the alkali and ethane will take place at high temperature, which is given by

$$6X + C_2H_6 \rightarrow 6XH + 2C \quad (7)$$

Here X is the alkali atom (K, Rb, or Cs) and XH is the corresponding alkali hydride. The deposition of XH and C will induce the degradation of cell windows transmission, and result in the increase of lasing threshold and the reduction of the output power [37]. This problem can be eliminated by buffering the alkali vapor with pure He. In this case, He is acting as both the spin-mixing and the pressure broadening gas. As listed in Table 4, the hydrocarbon-free DPAL has been realized experimentally for K and Rb lasers. For Cs laser, the hydrocarbon-free approach is not applicable for the Cs–He fine-structure mixing cross section is too small.

2.2. Pumping structure in DPAL

Longitudinal and transverse pumping structures are mainly used for alkali-vapor lasers. Longitudinal pumping is adopted in most DPAL for it is easy to obtain a relative high pump intensity and absorption efficiency, but it is difficult to achieve a higher output power for the thermal effect. Transverse pumping is convenient to couple multiple pump beams into the gain cell, and it is a preferred structure used in high power DPAL, but the gain distribution should be optimized and the output laser beam quality should be improved. To get a high power alkali laser with good beam quality, unstable cavity has been used in experiments.

2.2.1. Longitudinal pumping

Though the line-width of D2 transition can be broadened by buffer gas, it is still several times narrower than the emission line-width of LD. The pumping energy is not absorbed maximally by the alkali vapor yet. For this reason, longitudinal pumping structure is adopted to overcome the line-width disparity and achieve a higher absorbed-fraction of pumping energy. In this pumping structure, the opacity of the gain medium in the far spectral wings of the collisionally broadened D2 transition can be made sufficiently large, resulting in a high pump absorption efficiency [19].

A typical longitudinal pumping structure of DPAL is shown in Fig. 2. The linear polarized pumping beam is focused into the center of alkali-vapor cell by a telescope, where is also the position of oscillating laser beam waist. The alkali-vapor cell is placed in the oven to keep working temperature constant. Brewster windows at the ends of cell are set to minimize losses for oscillating laser, which is orthogonal polarized to pumping laser. A cube-type polarized beam splitter (PBS) is used to separate laser beam from pumping beam.

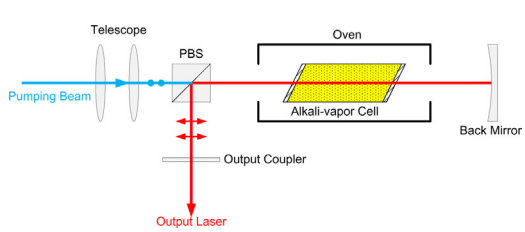

Fig. 2. Schematic diagram of a typical longitudinal pumping DPAL.

Two key issues should be concerned in the longitudinal pumping structure:

(1) Coupling the pumping laser into the gain cell efficiently and separating the oscillating laser from pumping laser.
Coating special films on dichroic mirror is usually used to reduce losses on pumping laser and separate the oscillating laser from pumping laser, but it is relative difficult for the minor wavelength difference between pumping laser and oscillating laser. Therefore, different polarizers are mostly used to getting orthogonal polarizations, such as PBS, thin film polarizer and so on [20,39].

(2) Optimizing the mode overlap between pumping laser and oscillating laser in the gain cell.
Mode overlap is the matching degree of the pump beam to the laser cavity mode, which is critical for the three-level gain medium since it creates reabsorption losses at the lasing wavelength when the pump beam size is less than the cavity mode size or waste of inverse population when the pump beam size is bigger than the cavity mode size [13,40]. There are several definitions on mode overlap [13,36,41], but all definitions are relative with the pump beam waist ω_P and oscillating laser beam waist ω_L. Experiments indicate that the mismatching between pumping laser mode and laser cavity mode exists in longitudinal-pumped DPAL all the time, an optimal mode overlap can be obtained experimentally by adjusting ω_P through different expansion telescope [13]. In the model of DPAL, mode overlap is introduced as an adjustable parameter to match the simulated results with the experimental results [36].

2.2.2. Transverse pumping

To scale up the output power of DPAL, the transverse pumping structure is used recently for its evident merits compared with the longitudinal pumping structure: (1) transverse pumping DPAL has a larger gain region generally, and it is promising to obtain high power laser output; (2) the pump laser and the oscillating laser are automatically separated, eliminating the need of sophisticated optics or complicated pumping geometries; and (3) the laser intensity on the laser windows is decreased, reducing less chance of optical damage. The development of transverse pumping alkali-vapor laser is listed in Table 5.

A typical transverse pumping DPAL is shown in Fig. 3. The alkali vapor cell is placed inside a cylindrical diffuse reflector which has a slit on its side paralleling to the cell axis. The diffuse reflector is assembled inside a temperature controlled oven. The pumping beam is coupled into cell by cylinder lens through the slit. The first transverse pumping DPAL is realized by using Cs as the gain medium, with an output power of 28 W and a slope efficiency of 15% [22]. The lower slope efficiency is attributed to low pump efficiency for the large disparity between cavity mode size and relative large reflector volume. As a result, a part of the pump radiation has

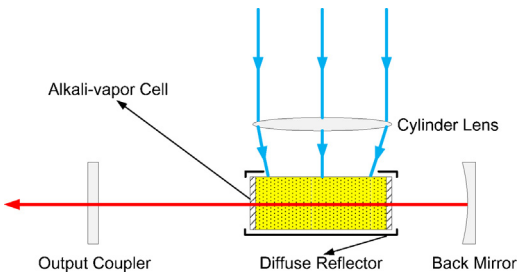

Fig. 3. Schematic diagram of a typical transverse pumping DPAL.

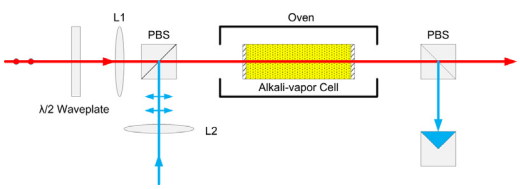

Fig. 4. A typical MOPA system of longitudinal pumping DPAL (λ/2 waveplate is used to adjust the input power).

not been used sufficiently. It is demonstrated that the slope efficiency can be improved by using an unstable cavity to increase the lasing mode volume. The slope efficiency is increased to 43%, and the output power is up to 49 W [15].

2.3. Power scaling of DPAL

Power scaling is one of the key techniques for DPAL, and the main technical difficulty is to realize higher output power and keep better thermal management simultaneously. One approach to realize high power DPAL output is a master oscillator power amplifier (MOPA), which allows simplifying the use of multiple pumping sources and handling the excessive heat released into the gain medium. MOPA system for DPAL has been investigated theoretically and its performance has been proved to be favorable experimentally [39,42–44].

As other MOPA laser systems, the DPAL MOPA system is also composed of two parts, one is the seed laser and the other is the amplifier, as shown in Fig. 4. The performance of MOPA is determined by its amplification factor

$$A = \frac{P_{out}}{P_{in}} = e^{gl} \tag{8}$$

Here P_{out} is the output power and P_{in} is the input power of seed laser, g is the gain coefficient and l is the length of gain cell.

The main issues influencing the amplification factor of the DPAL MOPA system mainly include the operating temperature, mode overlap between the pumping beam and seed laser, and pumping power. Experimental results indicate that the amplification factor increases with the operating temperature until it exceeds the optimal value, and it also increases with mode overlap and pumping power until appearing obvious thermal effects [39,42]. In addition, the incident power of the seed laser is also important for improving the MOPA performance. Experimental results [39,42] and theoretical model [44] show that the amplification factor is basically maintained at a constant for lower power of the seed laser. The MOPA is approaching the saturated regime when the seed laser increases to a certain value and it extracts nearly all the available stored energy in the gain medium. With the further increase of seed laser, the amplification factor begins to decrease, but the output power still increases. Therefore, it is necessary to keep a balance between the high output power and the efficiency when a DPAL MOPA system is designed.

A transverse pumping DPAL MOPA is realized with a maximum output power of 25 W and a maximum amplification factor of 10 [43]. It is demonstrated that the transverse pumping MOPA is more effective than the longitudinal pumping structure for power scaling of DPAL. The development of MOPA based on DPAL is listed in Table 6.

Another approach using a planar waveguide DPAL is also proposed to be a power-scaled system and the magnification performance has been studied theoretically [12]. The thermal effect can be mitigated by the reducing temperature gradient at the heat transporting direction in this approach.

3. Application of DPAL

3.1. Blue-violet Laser

High power blue-violet lasers are desirable for many applications, such as data recording, laser displays, underwater communication, laser medical treatment and environmental monitoring. One promising way to generate blue-violet lasers is frequency doubling of the DPAL.

Now, violet laser at 397.4 nm [45] and blue laser at 447 nm [46–48] are obtained by frequency doubling of Rb laser and Cs laser, respectively. By intracavity frequency doubling of Rb laser in BiBO crystal, 397.4 nm laser with output power of 250 mW and conversion efficiency of 1.5% is obtained from the fundamental laser [45]. 447 nm laser in PPKTP crystal is demonstrated, and continuous wave power of 600 mW with efficiency of 4% and peak power of 2.1 W with efficiency of 14% in pulsed operation are obtained, respectively [47]. Experimental results [48] of frequency doubling of Cs laser by using different nonlinear crystals are shown in Table 7.

In addition, a blue laser at 459 nm is also demonstrated by direct optical excitation to the $7^2P_{3/2}$ state of Cs vapor [24]. The corresponding pumping transition and lasing transition are $6^2S_{1/2} \rightarrow 7^2P_{3/2}$ and $7^2P_{1/2} \rightarrow 6^2S_{1/2}$, respectively. In this experiment, the Cs vapor cell is pumped by a pulsed 455 nm dye laser and the maximum output power is 500 mW.

3.2. Potential applications

DPAL can be the excellent light source for laser cooling and producing of the spin polarized noble atoms, where the narrow-line-width laser is required to be precisely detuned at specific hyperfine resonances. Therefore, DPAL can provide new approaches for researches on atomic physics, quantum optics and laser spectroscopy. In addition, DPAL has good beam quality and can be scaled up to high power, so it has great potential in laser directed energy applications, both civilian and military. For

Table 6
Development of alkali-vapor MOPA lasers.

Research, Year, Institute	Alkali	P_{pump} (W)	P_{in}	A
D.A. Hostutler, 2008, AFRL [39]	Rb	2.4	50 mW	6
B.V. Zhdanov, 2008, USAFA [42]	Cs	18	10 mW	145 (small signal)
B.V. Zhdanov, 2010, USAFA [43]	Cs	280	5 W	5
			0.5 W	10

Table 7
Frequency doubling performance in different crystals and different laser mode.

Geometry	Single pass extra-cavity frequency-doubling			Intra-cavity frequency-doubling		
Crystal	PPKTP	BiBO	LBO	PPKTP	BiBO	LBO
CW						
$P_{SH\text{-}max}$ (mW)	0.132	0.275	0.344	1240	218	90
$P_{f\text{-}max}$ (W)	5.0	5.4	3.9	10.3	17.8	21.7
Efficiency (%)	2.64	0.51	0.09	12.5	1.5	0.41
QCW (pulse width = 100 μs)						
$P_{SH\text{-}max}$ (mW)	594	30.8	11.4	2490	1120	277
$P_{f\text{-}max}$ (W)	4.4	5.3	5.3	10.8	16.6	15
Efficiency (%)	13.5	0.58	0.21	23.1	6.7	1.8

Annotation: $P_{SH\text{-}max}$ is the maximum power of the second harmonic laser and $P_{f\text{-}max}$ is the maximum fundamental laser power measured before incident the nonlinear crystal.

example, it is significant to transfer ground-generated power of DPAL to remote PV cells on satellites or space shuttles because DPAL offers high efficiency laser beams at the wavelengths matching with the absorption of PV cells, for example silicon cell at 895 nm (Cs laser), GaAs cells at 795 nm (Rb laser) and 770 nm (K laser). Furthermore, DPAL can be used in laser processing for its energy is easily absorbed by materials due to its shorter wavelength compared with Nd:YAG laser or CO_2 laser.

4. Prospects of DPAL

Researches on DPAL are mainly aimed at stable operation for high power output with good beam quality. The trend of DPAL is concluded from its key techniques.

(1) Hydrocarbon-free DPAL. Operating temperature is very high for high power DPAL, so it is easy to induce chemical reaction between the hydrocarbon gas and the alkali-vapor in long-time operation, and degrade the laser stability.
(2) Unstable cavity with transverse pumping structure. Efficiency of transverse pumping is not as high as longitudinal pumping, but it is more preferable to couple the pumping laser and improve the mode overlap by employing an unstable cavity.
(3) MOPA system of DPAL. To reduce the thermal effect, it is quite feasible to scale DPAL to higher power by adopting a chain of amplifiers.

5. Conclusion

In this paper, the development of DPAL is reviewed and the key techniques are summarized and analyzed in detail, including the interactions between buffer gas and alkali vapor, pumping structure and power scaling magnification. Novel techniques used in DPAL are discussed, such as hydrocarbon-free DPAL and unstable cavity with transverse pumping. Blue-violet lasers by frequency doubling of DPAL are also introduced specifically. Additionally, potential applications and the prospects of DPAL are concluded briefly.

References

[1] F. Chen, X. Yu, J. Gao, X.D. Li, R.P. Yan, J.H. Yu, Z.H. Zhang, 8.9-W continuous-wave, diode-end-pumped all-solid-state Nd:YVO_4 laser operating at 914 nm, Laser Phys. 19 (2009) 389–391.
[2] X.T. Yang, X.Z. Ma, W.H. Li, L. You, A narrow linewidth continuous wave Ho:YAP laser with a volume Bragg grating, Laser Phys. 21 (2011) 2080–2083.
[3] Z.C. Wu, All solid-state CW Nd:$GdVO_4$-GdCOB laser at 670 nm, Laser Phys. 21 (2011) 2068–2071.
[4] Y.L. Li, J.Y. Liu, Y.C. Zhang, T.Y. Zhang, T.Y. Ni, Z.H. Tao, All-solid-state Nd:YVO_4 laser at 1342 nm under 914 nm diode laser pumping, Laser Phys. 22 (2012) 343–346.
[5] S.T. Li, Y. Dong, C. Wang, B.Z. Li, Diode-pumped Nd:LGS laser emitting at 888 nm, Laser Phys. 22 (2012) 876–879.
[6] V.D. Bulacv, V.S. Gusev, S.Y. Kazantsev, High-power repetitively pulsed electric-discharge HF laser, Quantum Electron. 40 (2010) 615–618.
[7] S.Y. Kazantsev, I.G. Kononov, S.V. Pldlesnykh, K.N. Firsov, Electrode system for electric-discharge generation of atomic iodine in a repetitively pulsed oxygen-iodine laser with a large active volume, Quantum Electron. 40 (2010) 397–399.
[8] A.N. Panchenko, V.F. Tarasenko, Effective HF(DF) laser pumped by nonchain chemical reaction initiated by self-sustained discharge, Tech. Phys. Lett. 30 (2004) 454–456.
[9] A.A. Belevtsev, S.Y. Kazantsev, I.G. Kononov, A.A. Lebedev, S.V. Podlesnykh, K.N. Firsov, On stability of self-sustained volume discharge in working mixtures of non-chain electrochemical HF laser, Quantum Electron. 41 (2011) 703–708.
[10] W.F. Krupke, Diode pumped alkali laser, U.S. Patent No. 6,643,311.
[11] W.F. Krupke, R.J. Beach, V.K. Kanz, S.A. Payne, Resonance transition 795-nm rubidium laser, Opt. Lett. 28 (2003) 2336–2338.
[12] R.H. Page, R.J. Beach, V.K. Kanz, W.F. Krupke, First demonstration of a diode-pumped gas (alkali vapor) laser, in: Conference on Lasers and Electro-Optics (CLEO), Baltimore, MD, USA, 2005, p. CMAA1 (UV and Visible Lasers).
[13] B.V. Zhdanov, T. Ehrenreich, R.J. Knize, Highly efficient optically pumped cesium vapor laser, Opt. Commun. 260 (2006) 696–698.
[14] B.V. Zhdanov, C. Maes, T. Ehrenreich, A. Havko, N. Koval, T. Meeker, B. Worker, B. Flusche, R.J. Knize, Optically pumped potassium laser, Opt. Commun. 270 (2007) 353–355.
[15] B.V. Zhdanov, M.K. Shaffer, R.J. Knize, Cs laser with unstable cavity transversely pumped by multiple diode lasers, Opt. Express 17 (2009) 14767–14770.
[16] B.V. Zhdanov, M.K. Shaffer, R.J. Knize, Demonstration of a diode pumped continuous wave potassium laser, Proc. SPIE 7915 (2011) 791506–791511.
[17] J. Zweiback, A. Komashko, W.F. Krupke, Alkali vapor lasers, Proc. SPIE 7581 (2010) 75810G–75811G.
[18] Y.J. Zheng, M. Niigaki, H. Miyajima, T. Hiruma, H. Kan, High-efficiency 894-nm laser emission of laser-diode-bar-pumped cesium-vapor laser, Appl. Phys. Express 2 (2009) 032501–32511.
[19] W.F. Krupke, R.J. Beach, V.K. Kanz, S.A. Payne, DPAL: a new class of CW, near-infrared, high-power diode-pumped alkali (vapor) lasers, Proc. SPIE 5334 (2004) 156–167.
[20] B.V. Zhdanov, J. Sell, R.J. Knize, Multiple laser diode array pumped Cs laser with 48 W output power, Electron. Lett. 44 (2008) 582–584.
[21] B.V. Zhdanov, A. Stooke, G. Boyadjian, A. Voci, R.J. Knize, Rubidium vapor laser pumped by two laser diode arrays, Opt. Lett. 33 (2008) 414–415.
[22] B.V. Zhdanov, M.K. Shaffer, J. Sell, R.J. Knize, Cesium vapor laser with transverse pumping by multiple laser diode arrays, Opt. Commun. 281 (2008) 5862–5863.
[23] J. Zweiback, G. Hager, W.F. Krupke, High efficiency hydrocarbon-free resonance transition potassium laser, Opt. Commun. 282 (2009) 1871–1873.
[24] K.C. Brown, G.P. Perram, Cesium laser operating in the blue by direct optical excitation of the $7^2P_{3/2}$ state, Proc. SPIE 7915 (2011) 791507–791511.
[25] A.L. Shawlow, C.H. Townes, Infrared and optical masers, Physiol. Rev. 112 (1958) 1940–1949.
[26] S. Jacobs, G. Gould, P. Rabinovitz, Coherent light amplification in optically pumped Cs vapor, Phys. Rev. Lett. 7 (1961) 415–417.
[27] P. Rabinovitz, S. Jacobs, G. Gould, Continuous optically pumped Cs laser, Appl. Opt. 1 (1962) 513–516.
[28] B.A. Glushko, M.E. Movsesyan, T.O. Ovakimyan, Progresses of stimulated electronic Raman scattering and stimulated resonance emission in potassium vapor in the presence of buffer gas, Opt. Spectrosc. (USSR) 52 (1982) 458–459.
[29] Z. Konefal, M. Ignaciuk, Stimulated processes in sodium vapor in the presence of molecular buffer gas system, Opt. Quant. Electron. 28 (1996) 169–180.
[30] M.E. Movsesyan, T.O. Ovakimyan, S.V. Shmavonyan, Stimulated processes in a mixture of rubidium vapor and buffer gas under two-photon excitation, Opt. Spectrosc. (USSR) 61 (1986) 285–287.
[31] Z. Konefal, Observation of collision induced processes in rubidium–ethane vapor, Opt. Commun. 164 (1999) 95–105.
[32] S.S.Q. Wu, T.F. Soules, R.H. Page, S.C. Mitchell, V.K. Kanz, R.J. Beach, Hydrocarbon-free resonance transition 795-nm rubidium laser, Proc. SPIE 6874 (2008) 68740E–68741E.
[33] J. Zweiback, W.F. Krupke, 28W average power hydrocarbon-free rubidium diode pumped alkali laser, Opt. Express 18 (2010) 1444–1449.

[34] G.D. Hager, J. McIver, D. Hostutler, G. Pitz, G. Perram, A quasi-two level analytic model for end pumped alkali metal vapor laser, Proc. SPIE 7005 (2008) 700528–700531.
[35] G.D. Hager, G.P. Perram, A three-level analytic model for alkali metal vapor lasers: part I. Narrowband optical pumping, Appl. Phys. B 101 (2010) 45–56.
[36] R.J. Beach, W.F. Krupke, V.K. Kanz, S.A. Payne, End-pumped continuous-wave alkali vapor lasers: experiment, model, and power scaling, J. Opt. Soc. Am. B. 21 (2004) 2151–2163.
[37] B.V. Zhdanov, R.J. Knize, Diode-pumped 10W continuous wave cesium laser, Opt. Lett. 32 (2007) 2167–2169.
[38] J. Zweiback, A. Komashko, High-energy transversely pumped alkali vapor laser, Proc. SPIE 7915 (2011) 791509–791511.
[39] D.A. Hostutler, W.L. Klennert, Power enhancement of a rubidium vapor laser with a master oscillator power amplifier, Opt. Express 16 (2008) 8050–8053.
[40] X. Yan, Q. Liu, L. Huang, Y. Wang, X. Huang, D. Wang, M. Gong, A high efficient one-end-pumped TEM00 laser with optimal pump mode, Laser Phys. Lett. 5 (2008) 185–188.
[41] R.H. Page, R.J. Beach, V.K. Kanz, Multimode-diode-pumped gas (alkali-vapor) laser, Opt. Lett. 31 (2006) 353–355.
[42] B.V. Zhdanov, R.J. Knize, Efficient diode pumped cesium vapor amplifier, Opt. Commun. 281 (2008) 4068–4070.
[43] B.V. Zhdanov, M.K. Shaffer, R.J. Knize, in "High Energy/Average Power Lasers and Intense Beam Applications IV", Proc. SPIE vol. 7581 (2010) 75810F–75811F.
[44] B.L. Pan, Y.J. Wang, Q. Zhu, J. Yang, Efficient diode pumped cesium vapor amplifier, Opt. Commun. 284 (2011) 1963.
[45] A.B. Petersen, R.J. Lane, A diode-pumped Rb laser at 398 nm, Proc. SPIE 6871 (2008) 68711Q–68721Q.
[46] B.V. Zhdanov, Y.L. Lu, M.K. Shaffer, W. Miller, D. Wright, R.J. Knize, Frequency-doubling of a high power cesium vapor laser using a PPKTP crystal, Opt. Express 16 (2008) 17585–17590.
[47] B.V. Zhdanov, M.K. Shaffer, W. Holmes, R.J. Knize, Blue laser light generation by intracavity frequency doubling of Cesium vapor laser, Opt. Commun. 282 (2009) 4585–4586.
[48] B.V. Zhdanov, M.K. Shaffer, Y.L. Lu, B. Naumanm, T. Genda, R.J. Knize, Performance comparison of nonlinear crystals for frequency doubling of an 894 nm Cs vapor laser, Proc. SPIE 7846 (2010) 78460B–78461B.